Crystal structure and magnetoresistance of Na-doped $LaMnO_3$

1999 J. Phys.: Condens. Matter 11 1523

(http://iopscience.iop.org/0953-8984/11/6/016)

J. Phys.: Condens. Matter **11** (1999) 1523–1528. Printed in the UK PII: S0953-8984(99)97676-2

Crystal structure and magnetoresistance of Na-doped $LaMnO_3$

G H Rao†‡, J R Sun†, K Bärner‡ and N Hamad‡

† Institute of Physics & Centre for Condensed Matter Physics, Chinese Academy of Sciences, Beijing 100080, People's Republic of China
‡ IV. Physikalisches Institut der Universität Göttingen, Bunsenstrasse 11–15, D-37073, Göttingen, Germany

Received 18 September 1998

Abstract. The crystal structure and magnetoresistance of $La_{1-x}Na_xMnO_3$ ($0.05 \leqslant x \leqslant 0.20$) are investigated. $La_{1-x}Na_xMnO_3$ crystallizes in a rhombohedrally distorted perovskite structure and exhibits a sharp ferromagnetic transition as well as a negative magnetoresistance at around room temperature. On the basis of alternating-current susceptibility and resistivity measurements as well as a comparison with $La_{1-x}Sr_xMnO_3$ compounds, it is proposed that Na doping tends to drive the system from a regime characterized by strong Hund coupling and strong electron–phonon coupling to one characterized by weak Hund coupling and weak electron–phonon coupling.

1. Introduction

The perovskite manganese oxides $R_{1-x}A_xMnO_3$ (R = rare-earth metal; A = divalent element) have attracted considerable attention recently owing to their colossal-magnetoresistance (CMR) effects [1]. Study of the CMR effects in $R_{1-x}A_xMnO_3$ could benefit our understanding of strongly correlated electron systems. It was believed that the spin structure and electronic properties of $R_{1-x}A_xMnO_3$ were correlated via the double-exchange mechanism [2–4]. However, Millis *et al* argued that double exchange alone could not explain the CMR effects in $R_{1-x}A_xMnO_3$, and proposed that a strong electron–phonon coupling, e.g. via Jahn–Teller effects, should play an important role [5–7]. A magnetic and electronic phase diagram was established for $R_{2/3}A_{1/3}MnO_3$ to represent lattice effects [8, 9]. It was also shown that the tolerance factor was a key parameter in determining the magnetic and transport properties of the compounds, because it affects the bending of Mn–O–Mn bonds and therefore the one-electron bandwidth. Archibald *et al* suggested an unusual trapping out of mobile holes above T_c due to local, static Jahn–Teller deformation [10]. Up to now, most of the studies have concentrated on divalent-ion-doped $R_{1-x}A_xMnO_3$ compounds (A = Ca, Sr, Ba, Pb, etc) and most of the compounds investigated crystallize in an orthorhombically distorted perovskite structure (O′-type; $c/\sqrt{2} < a < b$; space group $Pbnm$) with a cooperative ordering of Jahn–Teller-distorted $Mn^{3+}O_6$ octahedra [11]. In contrast, there are few reports on perovskite manganates doped with monovalent alkali-metal ions [12]. Alkaline-earth-metal doping and alkali-metal doping of $LaMnO_3$ can lead to different consequences, e.g. the latter can lead to (i) less inhomogeneity, because fewer impurity ions (i.e. alkali-metal ions) are needed to achieve a specific carrier concentration, and (ii) larger random-potential fluctuations being experienced by the electrons in the σ^*-band, due to the larger difference in valence between

0953-8984/99/061523+06$19.50

La^{3+} and the alkali-metal ions [13]. In particular, it was reported that $La_yA_xMn_wO_3$ (A = Na, K, Rb) compounds crystallized in a rhombohedrally distorted perovskite structure without static Jahn–Teller deformations (space group $R\bar{3}c$) [12]. Therefore, the study of alkali-metal-doped perovskite manganates would offer significant complementary understanding of the CMR effects in these compounds. In this paper, we report on the crystal structure and magnetoresistance of sodium-doped $LaMnO_3$ compounds.

2. Experimental procedure

$La_{1-x}Na_xMnO_3$ bulk samples ($x = 0.05$, 0.10, 0.125, 0.15, 0.175, and 0.20) were prepared by a standard ceramic processing technique. Well mixed stoichiometric mixtures of La_2O_3, Na_2CO_3, and MnO_2 were calcined at 1273 K for 24 h. The powder thus obtained was ground, pelletized, and sintered at 1473 K for 96 h with an intermediate regrinding, then furnace cooled to room temperature. X-ray powder diffraction was carried out by using a Rigaku x-ray diffractometer with a rotating anode and Cu Kα radiation. The ac susceptibility between 77 K and ∼350 K was measured by means of a sensitive mutual-inductance method at a frequency of 320 Hz and in a low field of 0.4 mT. The resistance was measured by a standard four-probe method between 77 K and ∼350 K in magnetic fields of zero and 1 T, respectively.

Table 1. The final structural parameters of $La_{0.9}Na_{0.1}MnO_3$ (space group $R\bar{3}c$, $a = 5.5263(1)$ and $c = 13.3499(1)$ Å in a hexagonal setting, $R_p = 10.27\%$, $R_{wp} = 15.70\%$, $S = 1.32$).

Ion	Site	x	y	z	Occupancy
La^{3+}	6a	0.0	0.0	1/4	0.9
Na^{+}	6a	0.0	0.0	1/4	0.1
Mn^{3+}	6b	0.0	0.0	0.0	0.8
Mn^{4+}	6b	0.0	0.0	0.0	0.2
O^{2-}	18e	−0.5516(11)	0.0	1/4	1.0

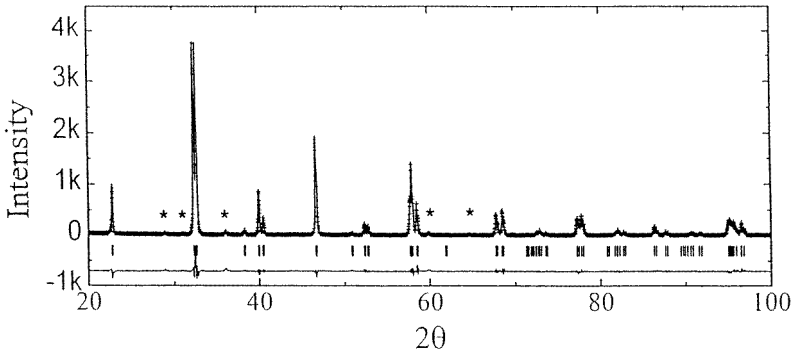

Figure 1. The XRD pattern of the compound $La_{0.9}Na_{0.1}MnO_3$. The observed data are indicated by crosses, and the calculated profile by a solid trace. The lowest trace shows the difference between the observed and calculated patterns. The vertical bars indicate the expected reflection positions. The asterisks denote the peaks from Mn_3O_4.

3. Results

X-ray powder diffraction (XRD) at room temperature shows that the synthesized samples are close to single phase with a small amount of Mn_3O_4 impurity phase. The amount of the impurity phase is estimated to be less than 5 wt% on the basis of XRD data, and no anomalies in the ac susceptibility and resistivity could be attributed to the impurity phase. The XRD pattern of the main phase can be indexed by a rhombohedral lattice with space group $R\bar{3}c$, which is consistent with the previous report on $La_yNa_xMn_wO_3$ compounds which were synthesized in O_2 flow [12]. The lattice parameters of $La_{1-x}Na_xMnO_3$ decrease linearly with x. The structural parameters were further refined by a standard Rietveld technique [14]. Figure 1 shows the observed and calculated XRD patterns of $La_{0.9}Na_{0.1}MnO_3$. The structural parameters are listed in table 1. In the refinement of the crystal structure, we tried to refine the occupancies of ions at (La^{3+}, Na^+) and (Mn^{3+}, Mn^{4+}) sites, but the refinement result was not significantly improved. Therefore, the nominal composition is tentatively taken as the composition of the compound, and the nominal Mn^{3+}/Mn^{4+} ratio was used in the Rietveld refinement. The structure of $La_{1-x}Na_xMnO_3$ is derived from the distortion of a primary cubic perovskite structure by rotations of MnO_6 octahedra along each (111) axis that release some internal stress due to the size mismatch of the ions (with tolerance factor $t < 1$). In contrast to the case for the orthorhombically distorted perovskite structure (O′ type), there is no buckling in the rhombohedral structure, the three Mn–O bonds are identical (=1.9660(2) Å for $x = 0.1$), the O–Mn–O bond angle deviates slightly from 90° (it is either 91.12(6)° or 88.88(6)° for $x = 0.1$), and the Mn–O–Mn bond angle (163.2(7)° for $x = 0.1$) is larger than that in the orthorhombic structure. Therefore, there are no static Jahn–Teller effects at room temperature in $La_{1-x}Na_xMnO_3$.

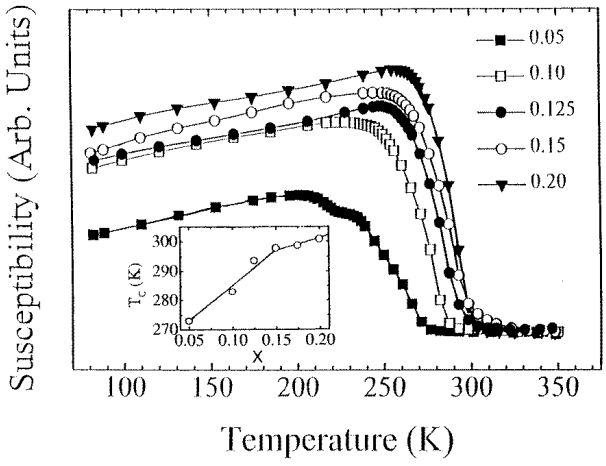

Figure 2. The temperature dependence of the low-field ac susceptibility of $La_{1-x}Na_xMnO_3$. The inset shows the composition dependence of the Curie temperature.

Low-field ac susceptibility measurement reveals a sharp ferromagnetic transition in $La_{1-x}Na_xMnO_3$ compounds (figure 2). The Curie temperature, T_c, increases linearly with x for $x \leqslant 0.15$, then levels off and increases at a slower rate (see the inset in figure 2). For the compound with $x = 0.05$, an anomaly is exhibited below T_c. Anomalies below T_c were also observed in the temperature dependence of the resistivity of some $La_yNa_xMn_wO_3$ compounds, and were considered to be an intrinsic characteristic of the compounds [12]. Since

the corresponding anomaly does not exist in $La_{1-x}Na_xMnO_3$ with higher sodium content, a contribution from the impurity phase cannot be the cause of the anomaly. Taking into account the fact that the anomaly occurs exclusively in the sample with the lowest sodium content, and the large difference in valence between La^{3+} and Na^+, which results in a large potential fluctuation experienced by the e_g electrons, it is plausible to attribute the anomaly to the existence of a magnetic inhomogeneity in the compounds [15, 16].

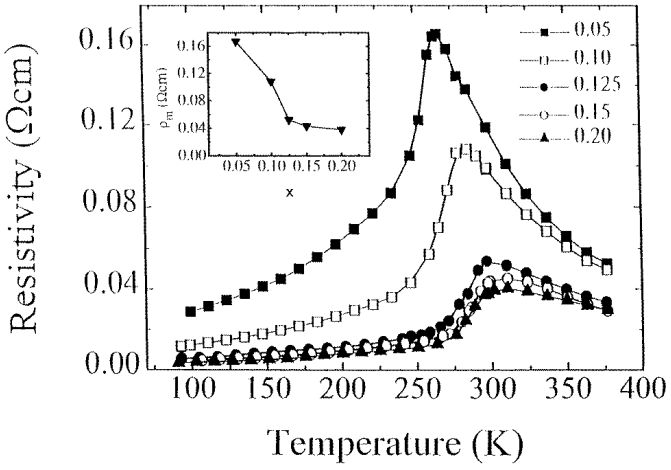

Figure 3. The temperature dependence of the resistivity of $La_{1-x}Na_xMnO_3$. The inset shows the dependence of the maximum resistivity, ρ_m, on the sodium content.

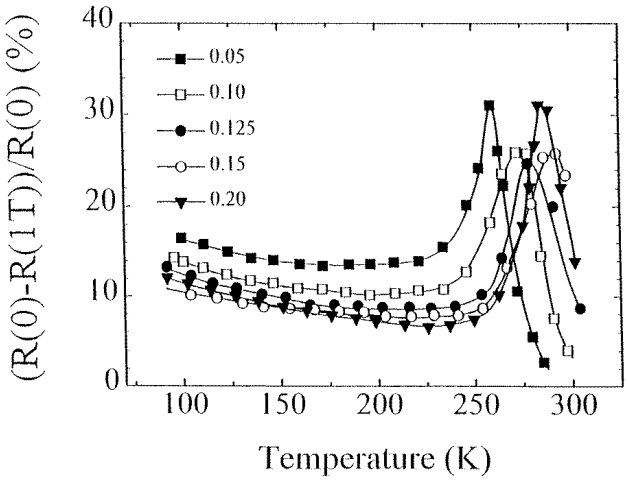

Figure 4. The temperature dependence of the magnetoresistance ratio of $La_{1-x}Na_xMnO_3$ at $H = 1$ T. The magnetoresistance was measured between 77 K and ∼300 K.

Figure 3 shows the temperature dependence of the resistivity of $La_{1-x}Na_xMnO_3$. A pronounced peak of the resistivity occurs at T_p ($\sim T_c$), indicating a metal–insulator (M–I) transition. The maximum resistivity, ρ_m, of the compounds decreases rapidly with the sodium content at lower x (see the inset in figure 3). As the sodium content increases further, ρ_m

decreases gradually and the rate of the resistivity decrease with temperature above T_c is reduced. When a magnetic field is applied, the resistivity of the compounds is decreased and the resistivity peak shifts to a higher temperature, leading to a negative magnetoresistance at around T_c. Figure 4 shows the temperature dependence of the magnetoresistance at 1 T, where the MR ratio is defined as $\Delta R/R = (R(1\ \mathrm{T}) - R(0))/R(0)$. For $x \leqslant 0.15$, the maximum MR at 1 T decreases with the increase of T_c, as reported for alkaline-earth-metal-doped $LaMnO_3$ [15,17]. In contrast, the maximum MR at 1 T seems to increase with T_c for $x > 0.15$.

4. Discussion

It is well known that the parent compound $LaMnO_3$ crystallizes in an orthorhombically distorted perovskite structure with a strong static Jahn–Teller distortion. Pure $LaMnO_3$ is an antiferromagnetic insulator associated with the large correlation energy of the d electrons in the e_g band. When divalent ions such as Ca^{2+}, Sr^{2+}, and Ba^{2+} substitute partially for trivalent La ions, hole doping occurs in the e_g band near the Fermi level, and ferromagnetism and metallic conductivity can be induced simultaneously in appropriately hole-doped compounds via the hopping of the e_g electrons [2–4]. It is instructive to compare the properties of $La_{1-x}Na_xMnO_3$ compounds with those of $La_{1-x}Sr_xMnO_3$ compounds. As the hole doping increases, the crystal structure at room temperature of $La_{1-x}Sr_xMnO_3$ changes from orthorhombic ($Pbnm$, $Z = 4$, $x < 0.175$) to rhombohedral ($R\bar{3}c$, $Z = 2$, $x \geqslant 0.175$) [18], and the Jahn–Teller deformation above the magnetic transition changes accordingly from static to dynamic. At $x \simeq 0.27$ the paramagnetic insulator (PI) $La_{1-x}Sr_xMnO_3$ changes into a paramagnetic metal (PM). Between $x = 0.175$ and 0.27, there is apparently a transition from strong Hund coupling between e_g and t_{2g} spins to weak Hund coupling [19]. In the weak-Hund-coupling region ($x > 0.27$), T_c for $La_{1-x}Sr_xMnO_3$ is less sensitive to an external pressure or to the change in bandwidth [19], and therefore changes only slightly with the tolerance factor or the bending of the Mn–O–Mn bond [8, 18]. In addition, it was argued that the PI-to-PM transition corresponds to a transition from a strong electron–phonon coupling, which gives rise to a high resistivity, to a weak electron–phonon coupling that favours a low resistivity [7]. All of these transients seem to be associated with the structural transition. Therefore, it is reasonable to speculate that the $La_{1-x}Na_xMnO_3$ compounds investigated, which crystallize in the rhombohedral perovskite structure, would be driven to a region of weak Hund coupling and weak electron–phonon coupling as the sodium doping increased. This picture seems to be supported by the observations that the increase of T_c and the decrease of ρ_m with x are more pronounced for $x \leqslant 0.15$ than for $x > 0.15$ (see the insets in figures 2 and 3), and that the rate of the decrease of resistivity above T_c is reduced as x increases. The transient character of the couplings is a plausible reason for the absence of a PI–PM transition in $La_{1-x}Na_xMnO_3$ ($x \leqslant 0.20$) and the anomalous relation between the maximum MR and T_c at higher sodium content.

While there has been extensive study of orthorhombically distorted perovskite manganate, the electronic and magnetic properties of the rhombohedrally distorted perovskite manganate are less frequently addressed. One of the obstacles might be the fact that the rhombohedral phase is obtained exclusively in $LaMnO_3$ that is doped with larger alkaline-earth-metal substitution in $LaMnO_3$—for example, in $La_{1-x}Sr_xMnO_3$ ($x \geqslant 0.175$) and $La_{1-x}Ba_xMnO_3$—i.e. the R phase seems to be associated with larger t [20]. The alkali-metal-substituted $LaMnO_3$ compounds provide an opportunity for a further investigation of the rhombohedral manganates with a smaller t (for the compounds that we investigated, t ranges from 0.910 to 0.927), which is of significance for an overall understanding of the CMR effects in perovskite manganate.

5. Summary

In summary, the crystal structure and MR properties of $La_{1-x}Na_xMnO_3$ compounds ($0.05 \leqslant x \leqslant 0.20$) have been investigated. It is proposed that a crossover from strong Hund coupling and strong electron–phonon coupling to weak Hund coupling and weak electron–phonon coupling occurs in $La_{1-x}Na_xMnO_3$; this seems to be related to the fact that the rhombohedrally distorted perovskite structure does not show static Jahn–Teller effects. To achieve a complete understanding of the CMR effects in the distorted perovskite manganates, further investigations of the perovskite manganates with structure distortions other than orthorhombic ones are necessary.

Acknowledgments

We would like to thank Mr X R Cheng for his assistance in the experiments. G H Rao is indebted to the Alexander von Humboldt (AvH) Foundation for a Research Fellowship. This project was partially supported by the Chinese Academy of Sciences (CAS).

References

[1] Jin S, Tiefel T H, McCormack M, Fastnacht P A, Ramesh R and Chen L H 1994 *Science* **264** 413
[2] Zener C 1951 *Phys. Rev.* **82** 403
[3] Anderson P W and Hasegawa H 1955 *Phys. Rev.* **100** 675
[4] de Gennes P-G 1960 *Phys. Rev.* **118** 141
[5] Millis A J, Littlewood P B and Shraiman B I 1995 *Phys. Rev. Lett.* **74** 5144
[6] Millis A J 1996 *Phys. Rev.* B **53** 8434
[7] Millis A J, Shraiman B I and Mueller R 1996 *Phys. Rev. Lett.* **77** 175
[8] Hwang H Y, Cheong S-W, Radaelli P G, Marezio M and Batlogg B 1996 *Phys. Rev. Lett.* **75** 914
[9] De Teresa J M, Ibarra M R, Garcia J, Blasco J, Ritter C, Algarabel P A, Marquina C and del Moral A 1996 *Phys. Rev. Lett.* **76** 3392
[10] Archibald W, Zhou J-S and Goodenough J B 1996 *Phys. Rev.* B **53** 14 445
[11] van Roosmalen J A M, van Vlaanderen P and Cordfunke E H P 1995 *J. Solid State Chem.* **114** 516
[12] Shimura T, Hayashi T, Inaguma Y and Itoh M 1996 *J. Solid State Chem.* **124** 250
[13] Coey J M D, Viret M and Ranno L 1995 *Phys. Rev. Lett.* **75** 3910
[14] Wiles D B and Young R A 1981 *J. Appl. Crystallogr.* **14** 149
[15] Rao G H, Sun J R, Liang J K and Zhou W Y 1997 *Phys. Rev.* B **55** 3742
[16] Sun J R, Rao G H, Liang J K, Shen B G and Wong H K 1997 *Appl. Phys. Lett.* **71** 3718
[17] Fontcuberta J, Martinez B, Seffar A, Pinot S, Garcia-Munoz J L and Obradors X 1996 *Phys. Rev. Lett.* **76** 1122
[18] Urushibara A, Moritomo Y, Arima T, Asamitsu A, Kido G and Tokura Y 1995 *Phys. Rev.* B **51** 14 103
[19] Moritomo Y, Asamitsu A and Tokura Y 1995 *Phys. Rev.* B **51** 16 491
[20] Radaelli P G, Marezio M, Hwang H Y and Cheong S-W 1996 *J. Solid State Chem.* **122** 444